16th World Conference on Earthquake, 16WCEE 2017

Santiago Chile, January 9th to 13th 2017

Paper N° 2360

Registration Code: S-P1463255766

ANALYSIS OF A SHEAR WALL REINFORCED CONCRETE BUILDING HEAVILY DAMAGED DURING THE 2010 CHILE EARTHQUAKE

C. Sepúlveda[1], G. Leiva[2]

[1] *Research Assistant, Universidad Técnica Federico Santa María, claudio.sepulveda.contreras@gmail.com*
[2] *Assistant Professor, Universidad Técnica Federico Santa María, gilberto.leiva@usm.cl*

Abstract

Correctly assessing the non-linear behavior of structural elements in buildings can improve the results of a seismic design. In this work, the most probable causes of the observed damage in a shear wall building during the 2010 Chile earthquake were detected by using two different approaches implemented in commercial software. The first procedure predicts the precise time in which the building gets into the nonlinear range by performing a linear elastic analysis. The second approach uses a fiber model to represent the inelastic response of specific wall zones, considering materials properties and the hysteretic behavior. The proposed model was validated with experimental results of rectangular and T-shape walls. The model enabled to obtain the nonlinear response of the entire structure and to compare it with the results of the linear analysis. The significant variation of the axial load on the elements analyzed, as well as the reduction of the shear and moment forces of the walls with respect to the linear model were studied. Disadvantages of the extrapolation of results obtained from a single axis simplification with respect to the behavior of the entire structure were examined. Results obtained have given insight about the observed type of failure in shear wall buildings.

Keywords: Nonlinear Analysis; Shear Wall Building; Inelastic Seismic Response; 2010 Chile Earthquake

1. Introduction

Currently most of the earthquake resistant structures are calculated using a modal spectral analysis based on a classic linear elastic model of the building, obtaining forces and displacements that afterwards are reduced by a factor that emulates the actual nonlinear behavior of the structural system. This methodology is based on the assumption that the inelastic behavior of the structure will be similar to the linear behavior, assumption that is not entirely correct.

Recent earthquakes in New Zealand (2011), Japan (2011), Chile (2010 and 2015) have revealed that shear walls buildings have a good performance when the design is based on an adequate seismic code (Wallace 2012 [1]). However, there is a little percentage of structures that failed, making necessary to introduce new tools and design philosophies that represent more accurately the real dynamic behavior of the structures on the nonlinear range over strong earthquakes to minimize the number of affected structures on future events.

2. Building studied

The analyzed structure is “Edificio Toledo”, a 10 story plus a subterranean level RC building, that was located in the city of Viña del Mar, Chile, and that suffered important damage during the 2010 earthquake. The building, designed in 1996, had to be demolished because the unfeasibility of its repairing. The plan distribution of structural walls at the first story is shown in Fig. 1. The extent of damage is shown in the same figure.

The main lateral force resistant elements in the Y-direction exhibited an important discontinuity of their sections at the first story, generating an increase of up to 260 cm (102´´) length from the 1st to the 2nd story, which means a 48% increase on the length of the wall. This discontinuity, commonly known as “flag wall”, is used to increase the usable space at the first floor and it was the main reason of the concentration of damage at this story.

The typical failure observed in the building is shown in Fig. 1, which was also seen in other structures during the 2010 Chile earthquake. Such failure is characterized by a large crack that completely extended along the wall length, with important damage of concrete and reinforcement on the borders of the cross section. The edge and some of the web longitudinal reinforcement showed buckling, and the stirrups, usually with 90° hooks, were open at the borders.

The most important damages occurred at the first story, in the main resistant elements in Y-direction. Minor cracking was observed in other stories and in the X-direction.

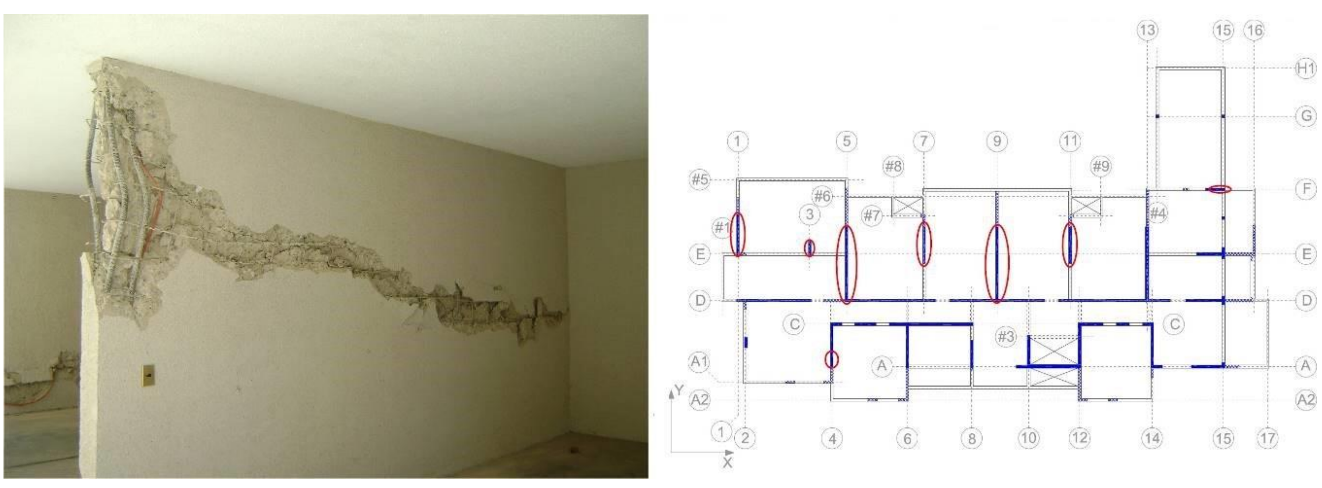

Fig. 1 – Damaged web of a T-shaped wall and a plane of the 1st story with the most important damages

3. Linear analysis

By using a 3D linear elastic model developed in the software ETABS, some analysis were made in order to give a framework which allows to understand how the 2010 Chile earthquake affected the studied structure. Considering uncracked section for the structural elements, the first mode is mainly rotational with a period of 0.69 seconds, the next mode is essentially in Y-direction with a period of 0.62 seconds and the third one is in X-direction with a period of 0.38 seconds. Every mode has a slight coupling between directions.

3.1 Analysis according to design codes

Using the ACI318-08 [2] and the Chilean actual seismic design code NCH433 [3], different regulatory aspects of the studied building were reviewed, by performing a reduced modal spectral analysis. Generally, there are no noticeable faults about displacement limits or building base shear. Regarding to critical elements, there are some walls with large axial force (greater than $0.35A_gf_c$’), and other elements subjected to forces outside of the nominal strength zone in the interaction diagram, but in the direction in which there was not damage, as it is shown in Fig. 2.

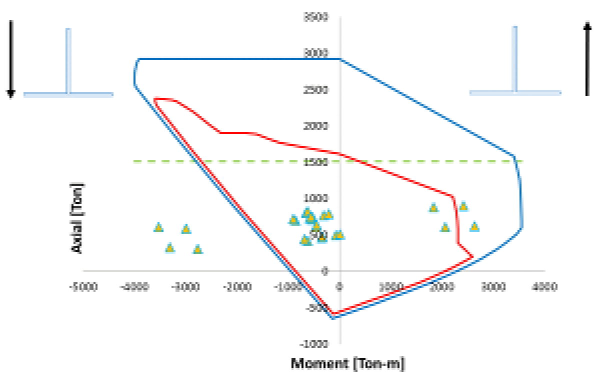

Fig. 2 – Interaction diagram for a T-shaped wall

Regardless of the faults, none of these are severe enough to be accounted for as a responsible for the important damage observed. However, in the actual Chilean design code a ductility verification is required to ensure that resistant elements could endure the displacement demand of the ground motion. This aspect is where most walls do not comply with code requirements. In Fig. 3, a moment-curvature plot of an analyzed wall is shown in continuous line, and the curvature demand in dashed line, revealing a grate ductility in one way, but a fragile behavior in the other, being unable to accomplish the demand.

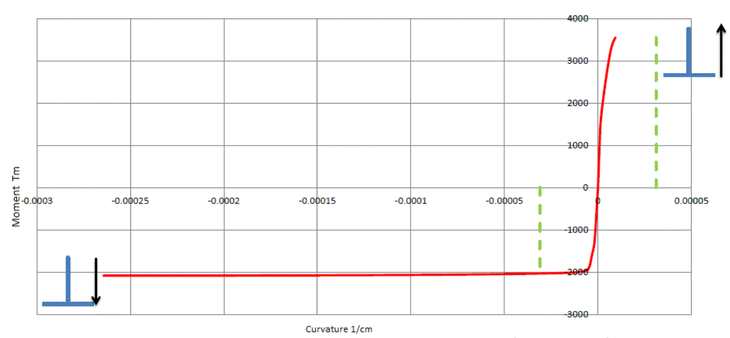

Fig. 3 – Moment-curvature of a T-shaped wall and the minimum curvature demanded

3.2 Time-history analysis

The modal spectral analysis of the seismic code uses a generic spectrum which depends on the soil type, seismic zone and other parameters. On the other hand, a time-history analysis gives more accurate results because it uses a specific seismic record measured close to the structure, giving a more appropriate representation of the dynamic building response. The record used here corresponds to the one obtained during the 2010 Chile earthquake in the "Viña del Mar Centro" station, located at 500 meters (0.3 miles) from the studied building. The record has a PGA of 0.33g, 0.22g, and 0.18g for the EW, NS and vertical directions, respectively. Fig. 4 shows the building base shear in Y-direction using only NS record (Y-direction) and both horizontal records, showing not significant differences between both responses. The same occurs in the X-direction, and for the roof displacement.

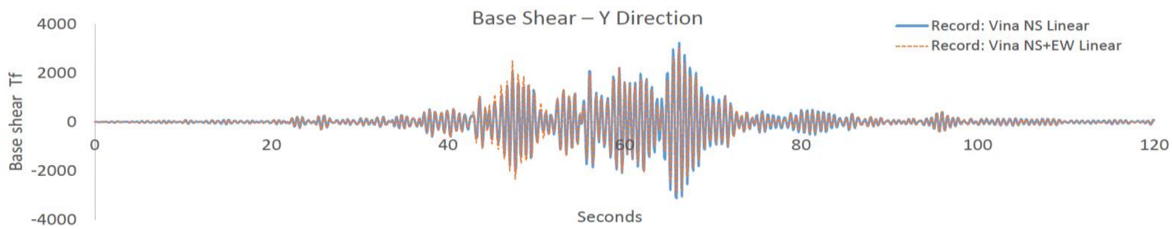

Fig. 4 – Base shear (Y-direction) using the NS record and both horizontal records

However, observing the roof rotation depicted in Fig. 5 a clear difference is observed when either one or both horizontal records are used.

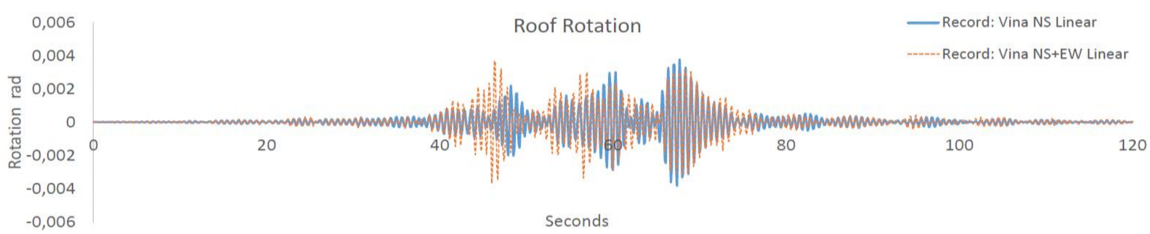

Fig. 5 – Building roof rotation using the NS record and both horizontal records

Such increase in the building rotation when both horizontal records are considered, affects the magnitude of forces received by the peripheral structural elements, as shown in Fig. 6. A clear increase in the axial load over the R1 wall is seen when both records are used, a behavior also found for moment and shear force over most walls. Finally, inclusion of the vertical component of movement in the analysis produces marginal changes.

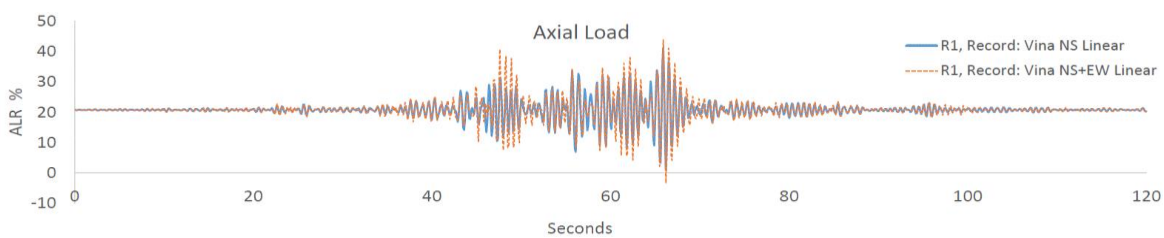

Fig. 6 – Axial load of element R1 (1st story) using the NS record and both horizontal records

By imposing to the studied building both horizontal components simultaneously and separately, it was found that, for some walls, an increase of 36% of the forces from the analysis with the perpendicular record must be considered to account for the behavior with both horizontal records, value which is close to the 30% suggested in some seismic codes.

4. First major event (FME) approach

A linear analysis loses its validity after the first inelastic incursion. However, it is possible to obtain important information from the linear model just before the first nonlinear incursion, which is when first major events happen. By knowing the instant in which the building starts to behave nonlinearly, it is possible to obtain an idea about the number of cycles in which the structure will respond in the inelastic range. Moreover, it could be possible to have information about which elements will generate such nonlinear behavior.

4.1 Description of method

An important event was defined as the occurrence of yielding in some of the most important structural elements. In order to detect these events, the curvature history of the main resistant walls at the first story and were compared with the yield curvature values. A time-history analysis was performed to a linear elastic model of the building by using the SAP2000 software, considering cracked sections. Because the axial load of each wall changes over time, the yield curvature will too. Therefore it is necessary to have an expression that enables to relate the yield curvature and the axial load over the wall. Afterwards, moment-curvature plots for different axial loads were generated, from which the yield and failure curvature were identified (Fig. 7). It must be emphasized that the yield curvature was defined as the value in which the steel rebar reach a strain value of 0.002.

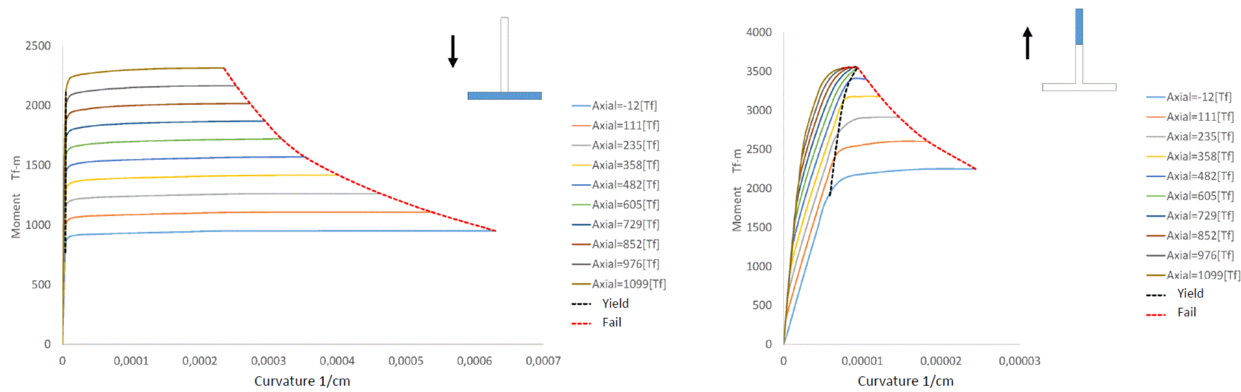

Fig. 7 – Moment-curvature for several axial load for both ways

Finally, in order to obtain the yield and failure curvature at any time, different curves were fitted for each load direction. For the yield curvature a straight line was fitted, getting $Ø_y(N)=\alpha N+\beta$, while for the failure curvature was utilized the expression $Ø_u(N)=\alpha(N+\gamma)^\beta$, with α, β y γ constants and N the axial load of the element. Thus, comparing the curvature of each wall with its yield curvature $Ø_y$ (or the failure curvature $Ø_u$) it is possible to obtain the instant in which each analyzed element has its first inelastic incursions.

4.2 Results of the method

With the purpose of getting a better result visualization, both element and failure curvature were normalized by $Ø_y$, so that when the normalized value of wall curvature reaches 1, the analyzed wall reached its yield curvature. In Fig. 8 the normalized curvature is presented in blue for the element "R1", in grey the $Ø_y$ value (1 or -1) and in red the normalized $Ø_u$. The graph shows that the element reached the inelastic range for the first time at 46.3 seconds in Y negative direction. A summary of the instants in which each element reached the nonlinear range is presented in Table 1.

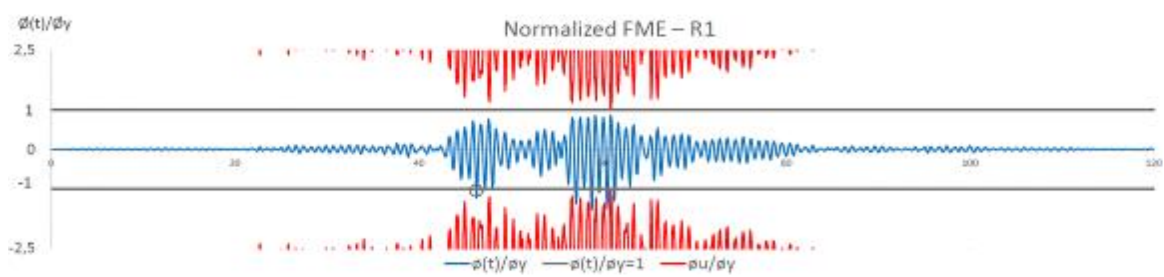

Fig. 8 – Normalized FME result for rectangular wall R1 in Y-direction ($Ø_{R1}(t)$: Blue; Øy: Grey; Øu: Red)

According to these results, elements responsible of the first major events during the earthquake were R1, L5 and L13, which reached the nonlinear range at 46 seconds approximately, time that corresponds to the beginning of the strong oscillations in the seismic record utilized. These findings show that the structure might had to withstand several cycles in the inelastic range. The accuracy of this method will be discussed later.

Table 1 – FME time for critical elements analyzed

Element	R1	R3	L5	R7	T9	R11	L13
FME time$^{(+)}$	-	-	60.9s	-	-	-	-
FME time$^{(-)}$	46.3s	-	46.3s	-	56.1s	56.2s	46.1s

5. Nonlinear analysis

In this last part of this work, a non-linear model for RC walls is proposed. That model will permit to obtain the nonlinear response of an entire building by using a commercial software.

5.1 Fiber model

The proposed method is based on a fiber model that represent the inelastic behavior of specific zones of reinforced concrete shear walls. In this case, the fiber model is applied only in the first story zone were the reduced section with concentrated damage is located. The rest of the building is modeled with linear elements. Because the proposed model is composed of several uniaxial fibers along the wall cross section, the interaction moment-axial load is implicitly included. Moreover, a curve to account for the shear behavior was included, but without an interaction with moment and axial load.

The fibers have a monotonic behavior curve, calculated according to the nonlinear properties of the concrete and the rebar steel considered into each one. The model of Mander et al. [4] was used for confined and unconfined concrete, without considering the tensile strength. A curve proposed by Belarbi et al. [5] was used for reinforcement steel, because this model gives a good representation of the behavior of a rebar embedded on concrete (Orakcal and Wallace, 2004 [6]). The curves used for both materials are illustrated in Fig. 9. For concrete, the two final points of the curve have the same stress in order to generate zero slope, since negatives slopes in the last segment lead to instabilities (Csi Analysis Reference Manual for Sap2000, 2013 [7]). The rebar curve has a non-zero slope after the yield stress, which corresponds to the Young's elastic modulus multiplied by a factor (b) equal to 0.002 (Polanco and Massone, 2013 [8]).

A curve for the shear behavior of each fiber is also included, by considering the expression used by Tuna and Wallace [9] which consist of 3 segments: the first one with a slope of 0.4 times the Young's modulus of concrete (E_c) until reaching the cracking shear force V_{cr}, then a slope of $0.01E_c$ until the nominal shear force V_n, after which the curve ends with a zero slope.

After performing a sensibility analysis, it was concluded the best option is to use 8 fibers or "link elements" in each wall, connecting each one to nodes of the shell elements.

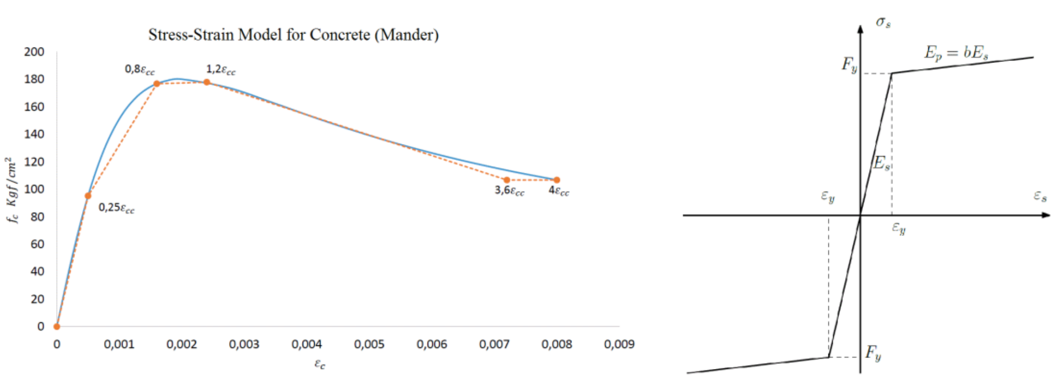

Fig. 9 – Stress-strain relationship for concrete and steel rebar

5.2 Calibration of the model with experimental results

Based on experimental data available in the literature, both plastic hinge length and the hysteretic behavior were determined. Firstly, data corresponding to cyclic tests of scaled rectangular walls with 3 different levels of axial load (15%, 25% and 35% of $A_g f_c$') carried out by M. Hube and J de la Llera [10] were used. The specimens were 10 cm (4'') thick, 70 cm (27.6'') long and 180 cm (71'') tall. The hysteretic law used was the Pivot model (Dowell et al., 1998 [11]), which requires to input the parameters α, β and η, which are related with the location of the Primary Pivot Point, the Pinching Point and the degradation of the elastic slope, respectively. Before performing the cyclic test simulation, it was necessary to add a rotational spring at the base of the wall to represent the additional rotation generated by the pedestal rotation effect. After testing several configurations, it was determined that the best results were made with a plastic hinge with a length of 75% of the wall length (L_w) and the hysteretic parameters indicated in the Table 2. In Fig. 10 the results of the wall response simulation are shown for an ALR=15%.

Table 2 – Plastic hinge length and parameters for hysteretic model (rectangular walls)

ALR	L_p	α_1	α_2	β_1	β_2	η
15%, 25% & 35%	$0.75L_w$=52.5cm (20.7'')	20	20	0.6	0.6	0

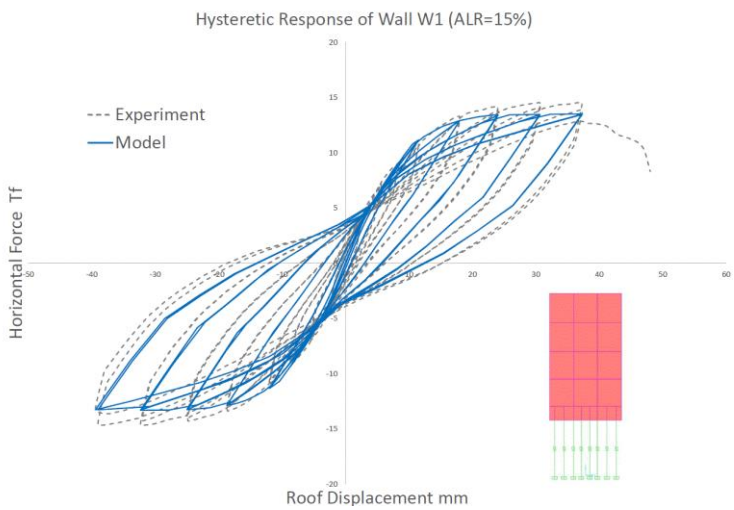

Fig. 10 – Hysteretic response of rectangular wall: Model vs. experiment data

Having these parameters selected, a nonrectangular wall response simulation was executed. For such simulation, tests of T-shaped walls carried out by Thomsen and Wallace [12] were utilized. The wall had 3.66 m (144'') height, 102 mm (4'') thickness and 1.2 m (44'') length, both for the web and the flange. Borders were confined and the tests were carried out with an axial load of 76 Tf, equivalent to ALR=7.5%. The author gives hysteretic curves without the shear and pedestal rotation components, so in the model only the bending component was considered.

For nonrectangular walls, a plastic hinge length of $0.5L_w$ in the web was considered in order to avoid extending the inelastic zone over one story. Besides, for flanges a plastic hinge length between 0.33 and $0.4L_w$ was considered so that the nonlinear fiber height was the same in both web and flanges. With the purpose of correcting such change in L_p respect to the value obtained with rectangular tests, a factor of 1.1 was applied at the Y values of the hysteretic behavior curve (force) of each fiber, which gives a similar behavior with respect to the $L_p=0.75L_w$ model used for rectangular walls simulations. Moreover, the Bernoulli assumption is not satisfied with nonrectangular walls about the strain profile. The model shows increased stiffness with respect to the experimental data since the flanges shows less deformation than expected (Orakcal and Wallace, 2006 [13]). In order to reduce the gap between the fiber model and the experimental response, and trying to does not affect the behavior in the flange direction, the X values of the hysteretic curve (displacement) of each fiber were amplified by 3, and also the factor 1.1 was changed by 0.5 for compression force (F_f(-)), producing the factors shown in Table 3. Results of the modeling with such parameters is showed in the Fig. 11.

Table 3 – Plastic hinge length and parameters for hysteretic model (nonrectangular walls)

ALR	L_p	α_1	α_2	β_1	β_2	η	F_f(-)	F_f(+)
Flange	-	20	20	0.6	0.6	0	1.1	1.1
Web	X3	20	3.3	0.1	0.6	0	1.1	0.5

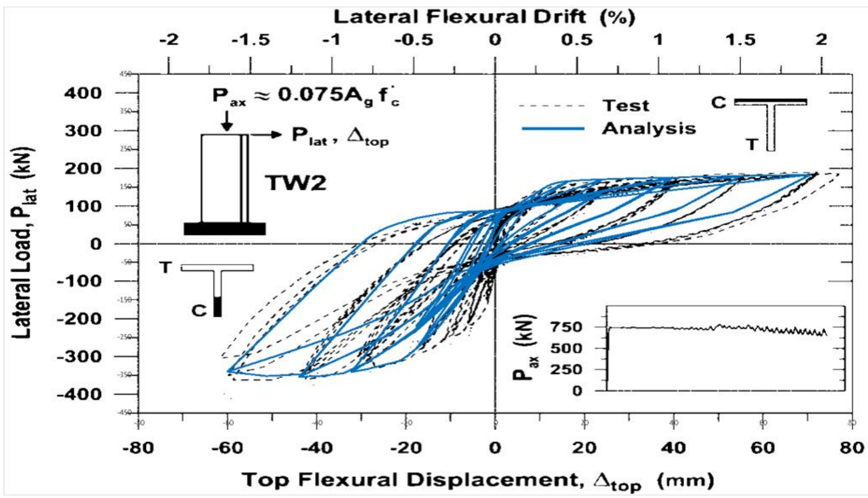

Fig. 11 – Hysteretic response of T-Shapped wall: Model vs. experiment data (Graph by Thomsen & Wallace)

6. Nonlinear building response

The nonlinear fiber model was incorporated in the most important elements at the first story of the building, allowing to model the nonlinear behavior of the whole structure. The three components of the record previously used were considered to obtain the dynamic response.

6.1 Global and critical elements response

Important differences are not observed in terms of both base forces and roof displacements by comparing the linear and nonlinear behavior. Although there is a slight phase shift between the biggest peaks, its magnitudes are very close. A comparison between the linear and nonlinear response for the base shear force and the roof displacement in Y-direction is shown In Fig. 12.

However, the reduction of the peaks is not perceived for the axial loads over the walls. On the contrary, an amplification of the magnitude of the highest peaks was observed. Analyzing the other elements, the same behavior is recurrent for the shear and moment forces, but the axial load can be either amplified or reduced with respect to the linear response, depending to the element analyzed.

All walls that incorporate this nonlinear fiber model reached a compression deformation greater than 0.003 in the concrete, and a tensile deformation greater than 0.002 in the steel rebar, with the exception of element L13, which was the only wall that had not visible cracking after the earthquake. It is important to highlight that such wall was the only one with a thickness of 25 cm at the first story, which represents 5 centimeters more than the other walls.

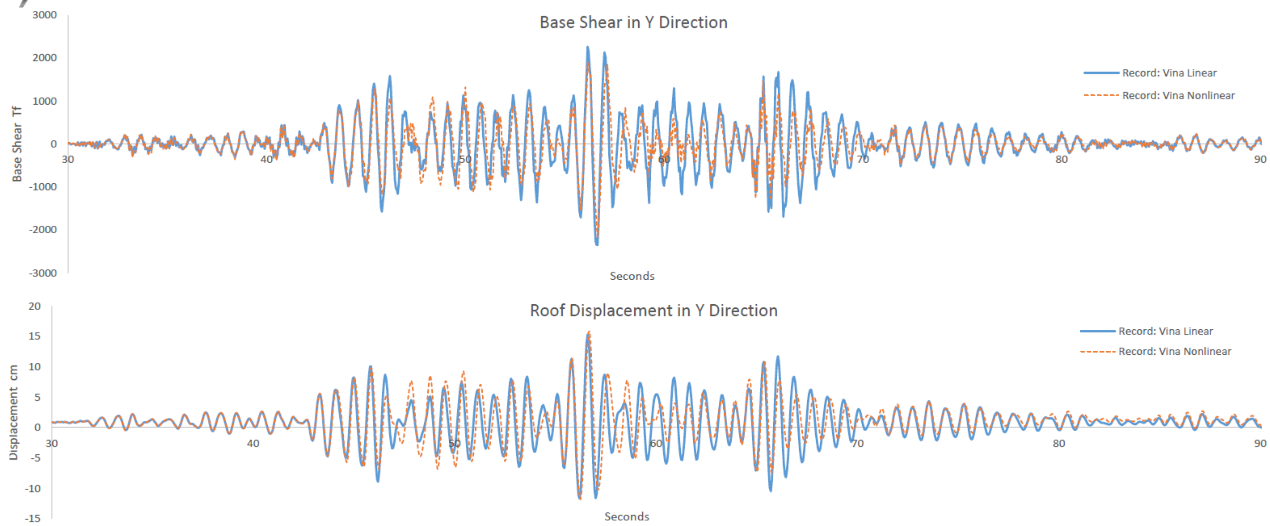

Fig. 12 – Comparison between linear and nonlinear global response: Base shear and roof displacement

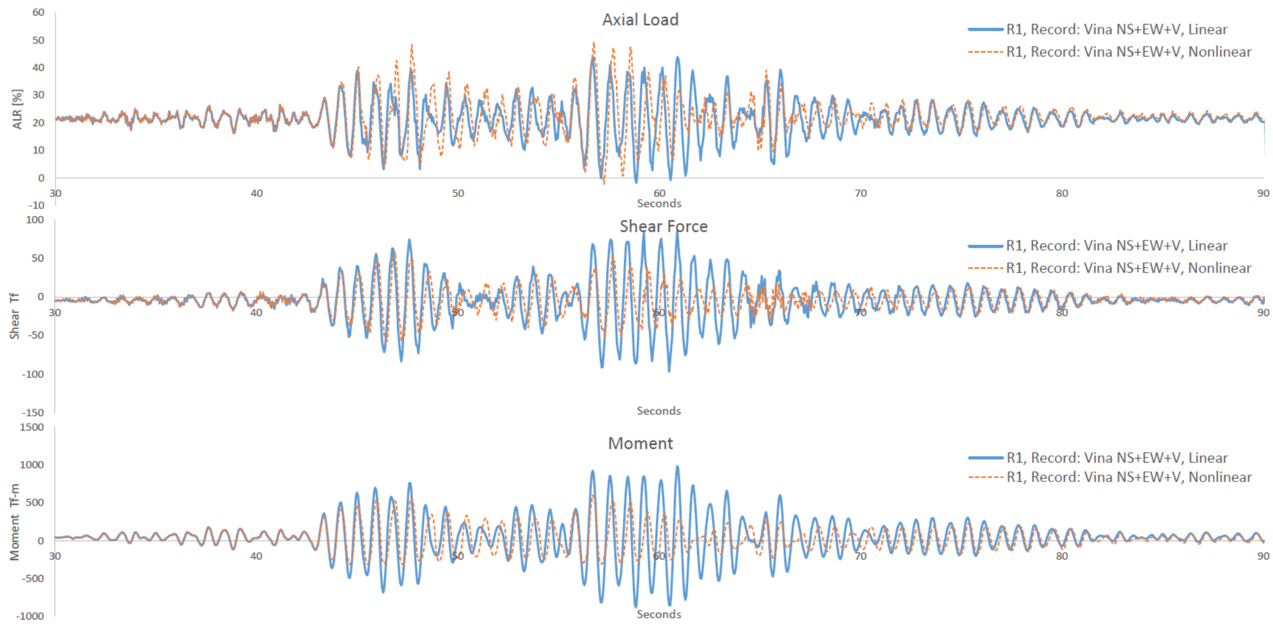

Fig. 13 – Comparison between linear and nonlinear response of forces over element R1

6.2 Nonlinear response vs. FME analysis

Having the nonlinear response of the structure, it is possible to analyze the effectivity of the FME approach proposed in this work. Fig. 14 depicts the linear and nonlinear base shear response in Y-direction and the roof rotation of the building. Within these plots the instants that the FME analysis identified as the first major events or first inelastic incursions of every wall are indicated.

It is observed that the proposed approach can identify properly the instants when the structure starts to behave nonlinearly, instants defined by the first times when both linear and nonlinear curves begin to separate from each other. However, when the responsible elements of these first nonlinear incursions are analyzed, the FME approach does not show a good correlation with the nonlinear analysis. In particular the FME approach indicates that the first elements incurring in inelastic behavior are R1, L5 and L13 at 46.3 seconds, but observing the hysteresis curves of each analyzed wall at this time, it is appreciated that the element R1 indeed has an important nonlinear behavior but, on the other hand, there are some walls with greater inelastic incursion than elements L5 and L13.

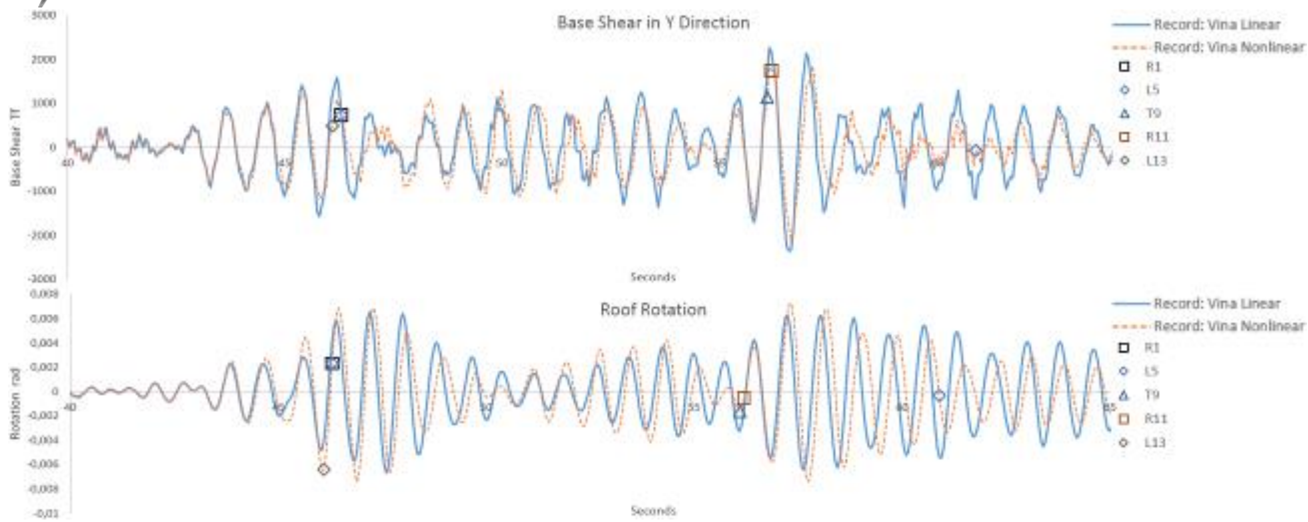

Fig. 14 – Analysis of accuracy of the FME approach proposed

6.3 Entire structure vs. single axis response

When a nonlinear model of a structure is required, sometimes just a part of the structure is modeled in order to be able to work with a less computationally demanding model. To analyze the accuracy of this approximation, two axis of the building with different characteristics were used: the axis 1, located at one end of the structure, which has a rectangular wall (R1) as the main resistant element; and also the axis 9, located at the center of the building, which has a T-shaped wall as the main resistant element. The seismic mass considered in the simplified model was modified in order to get the same main period of the entire building, aiming to obtain similar dynamic characteristics as the whole structure.

The dynamic response of the simplified model and the entire structure were compared by analyzing both linear and nonlinear responses. Analyzing the element R1 it is observed that the single axis simplification gives relatively close results in the linear and nonlinear model, in terms of axial load and moment at the base. However, by considering a linear analysis, the shear force in the single axis model is importantly amplified respect to the entire structure response, a difference that is increased when a nonlinear analysis is considered. In Fig. 15 the axial load and shear force of R1, considering inelastic behavior of the single axis model and the entire structure model, is presented.

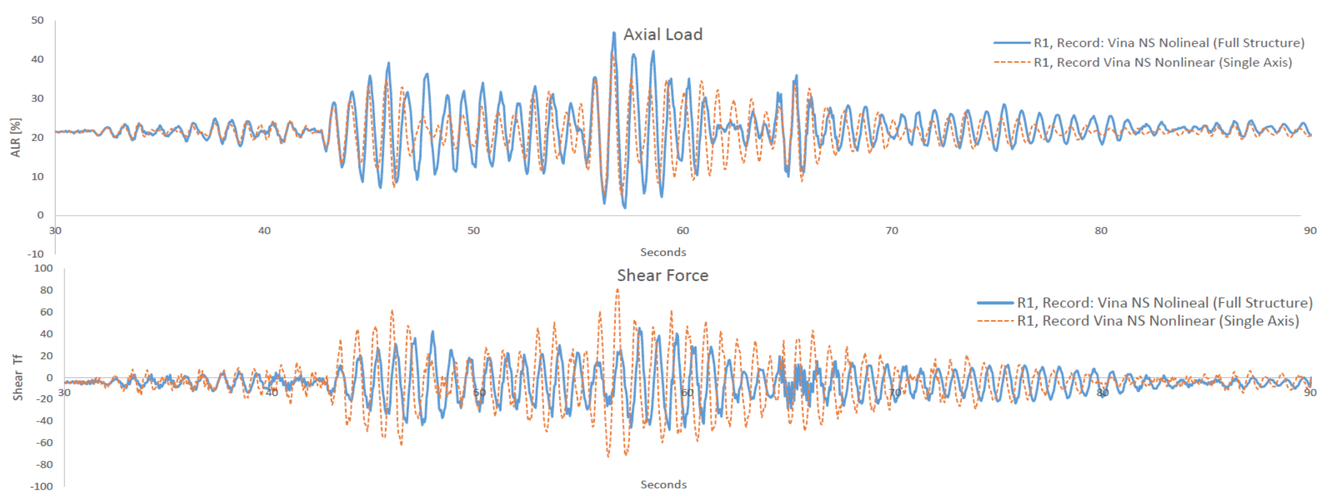

Fig. 15 – Axial load and shear force over element R1 using the nonlinear model: Entire structure vs. single axis

On the other hand, a different behavior is observed for element T9, which shows an important increase of the axial load to be used in the simplified model, behavior also found for the shear force but with lower amplification. In Fig. 16 the axial load and shear force of the element T9 are showed considering a nonlinear behavior.

From the previous figures it can be concluded that, depending on the element analyzed, the simplified model can amplify or reduce the force response with different levels of significance with respect to the results for an entire structure model, without the presence of a clear trend. Even though the linear analysis shows a similar behavior than the nonlinear analysis respect to amplifying or reducing the single axis response, their magnitudes differ. Therefore, it is difficult to obtain the nonlinear response of the entire structure by extrapolating the responses of the single axis nonlinear model, together with both single axis and entire structure linear models.

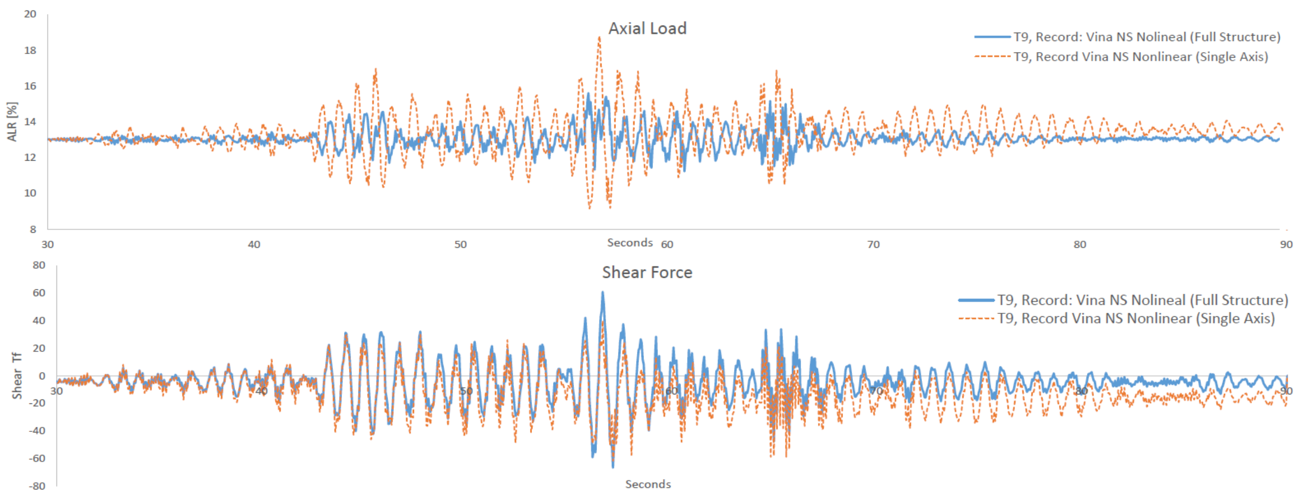

Fig. 16 – Axial load and shear force over element T9 using the nonlinear model: Entire structure vs. single axis

7. Conclusions

In this work several aspects to consider in a time-history analysis were discussed. Regarding the simultaneous use of seismic records in normal directions, it was determined that when a building has an important component of rotational modes, the structural element response can change significantly if one or both horizontal components of the movement are considered. Some seismic codes require to add 30% of the response from the perpendicular direction analysis, which is consistent with the 36% required increase obtained for the structure and record used in this work.

In this work, two approaches were proposed to obtain information about the dynamic behavior of a structure during a strong earthquake. The first one, FME, allows to identify the instant when the structure enters into the inelastic range, giving information about the number of nonlinear cycles that the building will be subjected. Besides, the effectivity of such approach to determine the structural elements that are responsible for the first nonlinear behavior was discussed, concluding that it is necessary to improve the methodology to obtain more reliable results.

The proposed approach to obtain the nonlinear response of reinforced concrete shear wall buildings, based in a fiber model concentrated in the expected inelastic zone, showed good results. The advantages of this method relies in the possibility to obtain a good approximation of the inelastic response of the entire building and the inelastic deformations in the borders of the walls, while carrying a reduced cost computational analysis by using a commercial software well known by the structural engineering community. It was found that, for the structural elements, both shear and moment forces show a reduction in the magnitude of their peaks when the building has a nonlinear behavior. However, the axial load over the walls does not show a clear trend, having amplifications even in the nonlinear response peaks. For this reason it is necessary to further research about the axial load over reinforced concrete shear walls over strong earthquakes, because a reduction of the axial load from a linear analysis is neither a good approximation nor a conservative assumption, since increasing the axial load reduces the ductility of the elements. Finally, this method helped to determine that by considering a simplified model of only a single axis of the entire structure does not produce good approximation of the nonlinear response, particularly with respect to wall forces.

In general terms, the principal causes of the failure of the analyzed structure, during the 2010 Chile earthquake, were some repeated patterns in the engineering designs, which became widely accepted after the good perform that structures had during the 1985 Chile earthquake. On one side, vertical irregularities in walls (“flag walls”) produce a concentration of nonlinear behavior reducing their ductility, which is an important feature to account for good seismic performance. Other observed feature, both in this building and in others damaged structures, was the wall’s reduced thickness and the lack of effective confinement at the wall borders, which further reduces the wall ductility and, thereby, the nonlinear cycles that the building can withstand. Proof of this is that the only important wall that did not have visible cracking was also the only wall 5 centimeters thicker than the rest, a behavior also observed in the nonlinear response determined in this work. The importance of the rotational modes was another important characteristic found for the studied structure. These rotational modes intensify the demand over the structural elements farther from the center of the building.

8. Acknowledgements

The authors of this paper would like to acknowledge to the professors Matías Hube and Juan Carlos de la Llera for providing the experimental data they obtained at the Pontificia Universidad Católica de Chile.

9. References

[1] John W. Wallace. Performance of Structural Walls in Recent Earthquakes and Tests and Implications for US Building Codes, 15th World Conference on Earthquake Engineering, 2012.

[2] ACI Committee 318, American Concrete Institute, and International Organization for Standardization. Building Code Requirements for Structural Concrete (ACI 318-08) and Commentary. American Concrete Institute, 2008.

[3] Nch433 of 1996 mod 2009+DS61 - Diseño sísmico de edificios, 2011

[4] J Mander, M Priestley, and R. Park. Theoretical stress-strain model for confined concrete. Journal of Structural Engineering, 114, 1988.

[5] Belarbi, Zhang, and Hsu. Constitutive laws of reinforced concrete membrane elements. 11th World Conference on Earthquake Engineering, page 1208, 1996.

[6] Kutay Orakcal and John W. Wallace. Modeling of slender reinforced concrete walls. 13th World Conference on Earthquake Engineering, paper No. 555, 2004.

[7] Csi Analysis Reference Manual for Sap2000, Etabs and Safe. Computers & Structures, 2013.

[8] J. Polanco and L. Massone. Estimación del desplazamiento lateral elástico e inelástico de muros esbeltos mediante un modelo de rótula plástica basado en un modelo de fibras. Memoria, Departamento de Ingeniería Civil, Universidad de Chile, 2013.

[9] Zeynep Tuna and John W. Wallace. Collapse assessment of the alto rio building in the 2010 chile earthquake. Earthquake Spectra, 0(0), 2014.

[10] M.A. Hube, A. Marihuén, J.C. de la Llera, and B. Stojadinovic. Seismic behavior of slender reinforced concrete walls. Engineering Structures, 80:377 – 388, 2014.

[11] Robert K. Dowell, Frieder Seible, and Edward L. Wilson. Pivot hysteresis model for reinforced concrete members. ACI STRUCTURAL JOURNAL, 95:607–617, 1998.

[12] John H. Thomsen and John W. Wallace. Displacement-based design of slender reinforced concrete structural walls - experimental verification. Journal of Structural Engineering, 130(4):618–630, 2004.

[13] Kutay Orakcal and John W.Wallace. Flexural modeling of reinforced concrete walls – experimental verification. ACI STRUCTURAL JOURNAL, 103:196–206, 2006.